Liquid Crystals

Publication details, including instructions for authors and subscription information:
http://www.informaworld.com/smpp/title~content=t713926090

Dielectric spectroscopy of a smectic liquid crystal

Shyamal Kumar Kundu[a]; S. Yagihara[a]; A. Yoshizawa[b]
[a] Department of Physics, School of Science, Tokai University, Hiratsuka, Kanagawa-259-1292, Japan [b] Department of Materials Science and Technology, Faculty of Science and Technology, Hirosaki University, Hirosaki 036-8561, Japan

To cite this Article Kundu, Shyamal Kumar , Yagihara, S. and Yoshizawa, A.(2007) 'Dielectric spectroscopy of a smectic liquid crystal', Liquid Crystals, 34: 8, 981 — 986

To link to this Article: DOI: 10.1080/02678290701541579

URL: http://dx.doi.org/10.1080/02678290701541579

Liquid Crystals, Vol. 34, No. 8, August 2007, 981–986

Dielectric spectroscopy of a smectic liquid crystal

SHYAMAL KUMAR KUNDU*†, S. YAGIHARA† and A. YOSHIZAWA‡
†Department of Physics, School of Science, Tokai University, 1117 Kitakaname, Hiratsuka, Kanagawa-259-1292, Japan
‡Department of Materials Science and Technology, Faculty of Science and Technology, Hirosaki University, Hirosaki 036-8561, Japan

(*Received 23 March 2007; in final form 14 June 2007; accepted 18 June 2007*)

Complex dielectric spectroscopy (frequency range 5 Hz–13 MHz) has been used to analyse the frequency, temperature and bias-field dependences of the molecular dynamics of a very high-spontaneous-polarization ferroelectric liquid crystalline material exhibiting SmA, SmC* and unknown SmX smectic phases. Different smectic phase transition temperatures have been observed from the study of the temperature dependence of the dielectric strength and the relaxation frequency. The phase transition temperatures (crystalline to isotropic phases) have also been described very accurately from the temperature-dependent symmetric and asymmetric shape parameters of the relaxation function and also the dc conductivity. In a planar aligned cell, two symmetric modes (Goldstone mode and domain mode) have been observed in both the SmX and SmC* phases. One asymmetric mode (X-mode) observed in the SmC* and SmA phases could be related to the interaction of dipoles of the ferroelectric liquid crystals being affected by the surface of the cell. The soft mode, which usually appears very close to the SmC*–SmA phase transition was not observed until the bias field was applied. The second order nature of the SmC*–SmA phase transition was revealed.

1. Introduction

The dielectric behaviour of ferroelectric liquid crystals (FLCs) is known to be complex. Since their discovery, they have attracted interest, not only in fundamental research but also for their important technological applications [1–3]. Clark and Lagerwall [4] showed the possibility of utilizing FLCs for electro-optical devices such as displays, memories and also for the synthesis of new FLC materials. Quite a number of new FLC materials have been discovered and their various properties have been investigated by different research groups using different methods [5–7].

Dielectric relaxation spectroscopy is one of the most basic and useful tools for investigating the molecular dynamics in FLCs, which are essentially electro-active. It is well known that study of the dielectric relaxation behaviour of LCs provides valuable information regarding the dipolar response to an external stimulus. The dielectric relaxation in the chiral smectic C (SmC*) phase occurs due to either collective dielectric processes (related to director reorientational motion) or the molecular reorientation processes connected with the polarization of the molecules. The main collective dielectric processes are due to the Goldstone mode (GM) [8–13] connected with the phase fluctuations in the azimuthal orientation of the director, and the soft mode (SM) [8–13] due to the fluctuations in the amplitude of the tilt angle. In FLCs with high spontaneous polarization (P_s), the structural parameters can be influenced by P_s under certain conditions (a new domain structure with different periodicity in the bulk and at the surface has been proposed). This collective dielectric process is known as the domain mode (DM) [9, 10, 14]. In the MHz region, the FLC exhibits two high-frequency molecular processes corresponding to the molecular rotation of the molecules around the long and short axes. These processes are present in all liquid crystalline phases and have been well reported [14–17].

It is generally considered that the SmC*–smectic A (SmA) transition is due to the softening of the particularly inhomogeneous fluctuations of the molecular tilt with respect to the normal to the smectic layer when the transition is approached from the SmA phase. In the ferroelectric phase, a spontaneous tilt of the molecules appears, the directions of which move in a procession about the smectic layer normal, a helicoidal structure being formed. As usual, the signature of the S-mode is indicated a few degrees above and below the SmC*–SmA-transition temperature [8, 13]. It is also

---

*Corresponding author. Email: sspskk@rediffmail.com

Liquid Crystals
ISSN 0267-8292 print/ISSN 1366-5855 online © 2007 Taylor & Francis
http://www.tandf.co.uk/journals
DOI: 10.1080/02678290701541579

well known that in the SmC* phase the S-mode can be detected only near the SmA–SmC* phase transition and when the G-mode is suppressed by a dc bias-field [12, 14, 16]. Otherwise it is overwhelmed by the G-mode.

A low-temperature smectic phase, called SmX (i.e. undefined), occurs in different substances with quite different phases [18–20]. It has a simple lamellar structure with a layer spacing of ~34 Å and it develops a spontaneous polarization on cooling. A plausible explanation of the reduced layer spacing in the SmX phase [21] is that the molecular axis is tilted with respect to the layer axis. There can, however, be no long-range order of the SmC type due to this tilt, in view of the optical uniaxiality of the phase. Some studies on the SmX phase have been undertaken, e.g. X-ray analysis [22], DSC [22, 23] and electro-optical analysis [24]. Some authors reported that the dielectric characteristic in the SmX phase of the FLCs is very poor [25]. Other authors reported that only the G-mode exists [26] in the SmX phase. However, a detailed analysis of the SmX phase by dielectric spectroscopy has not yet been undertaken.

In the present paper, we report the results of precise measurements of the temperature-dependent dielectric relaxation behaviour of a FLC material in different smectic phases. We also report the frequency-dependent dielectric relaxation behaviour in the different smectic phases. The effects of the bias field on the G-mode and the SmC*–SmA phase transition are investigated.

2. Experimental

The chemical structure of the FLC material studied is shown in figure 1.

The method of synthesis of this material has been described by Shiratori *et al.* [27]. This FLC material has the phase sequence: isotropic (I)→136°C→SmA*→132.5°C→SmC*→105°C→SmX→86°C→crystal (Cr). In this material, the SmX phase is in reality a partially crystalline phase. The molecular weight (M_w) of this FLC material is 493. The maximum spontaneous polarization in the SmC* phase is 438 nC cm^{-2}.

We investigated the dynamics of the FLC material with and without bias-voltage (0–15 V) for a cell of thickness 5 µm. The FLC material was sandwiched between the two ITO-coated glass plates separated by a mica spacer of 5 µm thickness. The glass plates were treated with a polyimide solution (PVA) and unidirectionally rubbed for planar alignment. The cells were first calibrated using air and toluene as the standard references. This allowed us to calculate the absolute value of the dielectric permittivity. The FLC material used in this study was inserted in the cell by capillary action in its isotropic phase. The cooling and heating cycles were continued several times for a better molecular alignment. The quality of the molecular alignment of this cell was checked using a polarizing microscope. During the dielectric measurement, the sample temperature between 80 and 140°C was controlled with an accuracy of ±0.1°C. The dielectric measurements were carried out by a computer-controlled HP 4192A impedance analyser having a frequency range of 5 Hz–13 MHz. The temperature, frequency and bias-field dependences of the real (ε') and imaginary (ε'') parts of the dielectric permittivity were determined from crystalline to isotropic phases and the experimental data were also analysed using theoretical models.

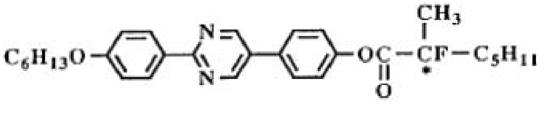

Figure 1. Chemical structure of the FLC material studied.

3. Results and discussion

The frequency dependence of the complex dielectric permittivity ($\varepsilon^*=\varepsilon'-i\varepsilon''$, where ε' and ε'' are, respectively, the real and imaginary parts of the dielectric permittivity) for the 5 µm thick sample of the FLC material at a fixed temperature of 107°C is shown in figure 2. From this figure, we observed four relaxation processes denoted as G-mode, D-mode, X-mode and the molecular rotation of the molecules around the long axis known as molecular (M) mode. It is well known that LCs are not absolutely free from impurities. The dc conductivity of the liquid crystalline materials is generally observed to be in the low-frequency side of the dielectric spectrum. We also observed this behaviour, as shown in figure 2.

To characterize all the relaxation processes, curve fitting procedures were carried out. The dielectric constant and loss for the present FLC material were determined from a fitting of the complex dielectric permittivity [14, 16] using

$$\varepsilon^*(\omega)=\sum_k \Delta\varepsilon_k(\omega)+\varepsilon_\infty+\frac{\sigma_{\mathrm{dc}}}{i\omega\varepsilon_0}, \qquad (1)$$

where $\Delta\varepsilon_k(\omega)$ accounts for the contribution of each mode, σ_{dc} is the dc conductivity, ε_0 is the dielectric constant in a vacuum and ε_∞ is the high-frequency permittivity. For $\Delta\varepsilon_k(\omega)$, we use the Havriliak–Negami function [28]:

$$\Delta\varepsilon_k(\omega)=\frac{\Delta\varepsilon_k}{\left[1+(i\omega\tau)^{\beta}\right]^{\alpha}}, \qquad (2)$$

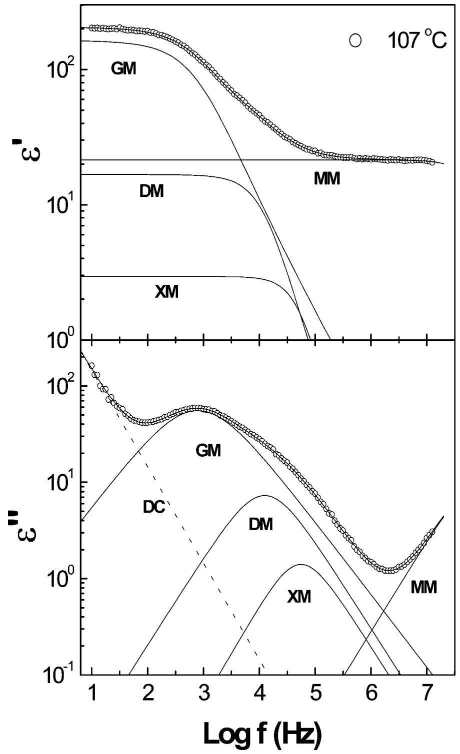

Figure 2. Frequency dependences of the real (ε′) and imaginary (ε″) parts of the dielectric constant in the ferroelectric SmC* phase at a fixed temperature of 107°C. The lines were drawn using equation (1). Dotted line: dc conductivity (DC). Solid lines: G-mode (GM), D-mode (DM), X-mode (XM) and M-mode (MM).

where $\Delta\varepsilon_k(\omega)$ is the dielectric strength, τ $(=1/2\pi\nu)$ is the relaxation time, ν is the characteristic frequency, and β and α are, respectively, the symmetric and asymmetric broadening parameters. $\alpha=1$, $\beta=1$ gives the Debye function; $\alpha=1$, $0<\beta\leqslant 1$ gives the Cole–Cole function; $\beta=1$, $0<\alpha\leqslant 1$ gives the Cole–Davidson function. In general, all these parameters are temperature dependent.

From the curve fitting procedures [14, 16, 29, 30], we observed from figure 2 that the G-mode (GM), D-mode (DM) and M-mode (MM) relaxations are symmetric and follow the Cole–Cole function. Here, it should be noted that the loss peak for the M-mode is observed in all the phases but it is outside the high-frequency limit of our experiment and only its low-frequency tail was observed, so that the relaxation parameter of the M-mode cannot be determined accurately. Only the X-mode (XM) is asymmetric and follows the Havriliak–Negami function. The dc conductivity in figure 2 is denoted by the dashed line. Here, GM and DM relaxations are very well known [9–17] but the X-mode observed in the present investigation is unusual. We observed the X-mode with asymmetric shape below the MHz region. The asymmetric shape of the dielectric loss curve has been observed for polymers [31] and aqueous mixtures of associated liquids [32], in which the chain motions and molecular motions follow the chain connectivity and the cooperative interaction between water and associated liquid molecules, respectively. One can find that, for high-spontaneous-polarization FLC materials, the molecular rotation around the molecular short axis appears in the MHz region [14, 16]. We expect that the appearance of the X-mode in the present investigation could be related to the dipoles of the FLCs interacting with the surface of the FLC cell, and this interaction depends on the molecular alignment.

The variation of the dielectric strength for the G-mode for the SmC* and SmX phases with temperature is shown in figure 3a. In this figure, a small jump can be observed at the SmC*–SmX phase transition region. This arises due to the reduced layer spacing in the SmX phase [21] when the molecular axis is tilted with respect to the layer axis. Figure 3b shows the variation of the dielectric strength for the D-mode and X-mode with temperature. From figure 3, we see that the G-mode and D-mode appear in the SmC* and SmX phases but X-mode appears in the SmC*, SmA and isotropic (I) phases. The S-mode, which is the signature of the SmA–SmC* phase transition, [8, 11–13] was not detected until the bias-field was applied because of the large contribution of the G-mode.

The variation of the relaxation frequency with temperature for all the phases (Cr to I phases) is shown in figure 4. Phase transition temperatures between the Cr and I phases are easily deduced from this figure. The different smectic phase transitions are also described very accurately from the plots of the dc conductivity (σ_{dc}), asymmetric (α) and symmetric (β) parameters for all the relaxation processes observed in the present FLC

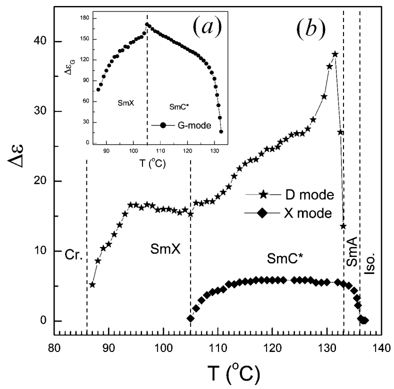

Figure 3. (a) Variation of dielectric strength (Δε) with temperature for G-mode in SmC* and SmX phases. (b) Variation of dielectric strength (Δε) with temperature for D-mode and X-mode for all phases.

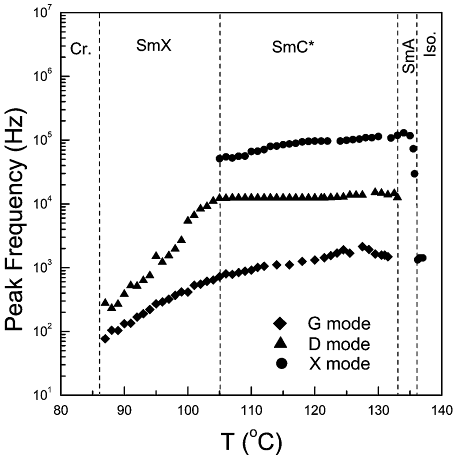

Figure 4. Variation of relaxation frequency with temperature for all phases.

material with temperature, as shown in figures 5. In the SmX phase, we observed that σ_{dc} increases rapidly with temperature. We expect that a very low-frequency process with very high dielectric strength could have occurred. However, this is very difficult to detect due to the low-frequency limit of our present experiment. Figure 5b shows the phase transition temperatures for the different smectic phases very accurately. The phase transition temperatures for the different smectic phases can be obtained from figure 5c, in which the change of β at the different smectic phase transitions is very small.

In the ferroelectric SmC* phase, the G-mode is strongly affected by the bias-field [12, 14, 16, 33, 34]. Figure 6 shows the bias-field dependences of the dielectric strength, relaxation frequency, dc conductivity, and symmetric and asymmetric shape parameters at a fixed temperature of 107°C in the SmC* phase. In figure 6a, we see that the dielectric strength increases, and then decreases rapidly and then is saturated. In figure 5b, the D-mode and X-mode also change in the same way as the G-mode. The dielectric strength first increases and then decreases when the bias-field is applied, due to the coercive field in the ferroelectric phase. The effect of the bias voltage on the relaxation frequency for the different relaxation processes is very small. The shape parameter α is almost constant when the bias-field is applied. When the bias-field is low, the β value decreases and then becomes independent of the voltage for the G-mode, D-mode and X-mode.

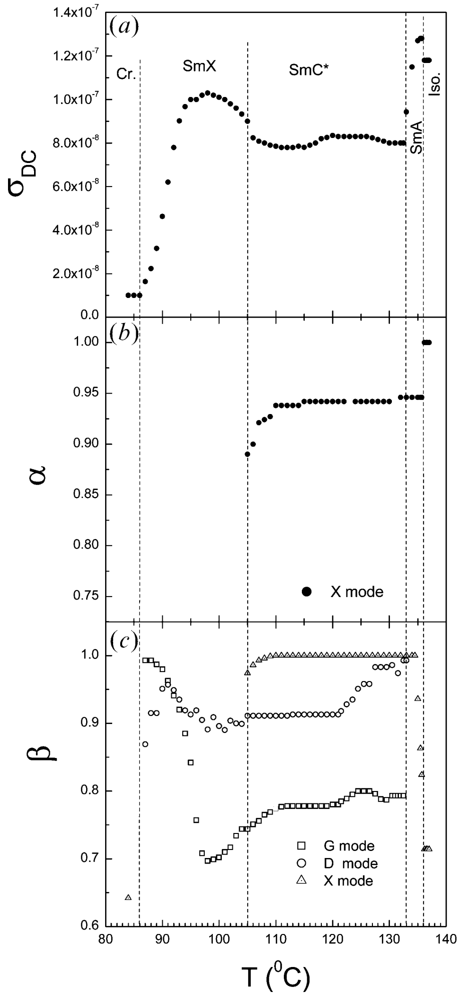

Figure 5. Variations of (a) dc conductivity (σ_{dc}), (b) asymmetric parameter (α) and (c) symmetric parameter (β) with temperature for all phases.

According to Levstik *et al.* [8] the S-mode in a FLC material can appear in both the SmC* and the SmA phases very close to the SmC*–SmA transition temperature. However, from figure 3, the S-mode could not be detected in the SmC* phase due to the large contribution of the G-mode. By applying a bias-field perpendicular to the helix axis, the SmC* phase loses the stability of its helical structure and the S-mode is detected in the SmC* phase. The bias-field causes a decrease in the G-mode with a corresponding increase in the S-mode character. Thus, to obtain the S-mode contribution for the SmC* phase, the effect of the bias-field is necessary for this sample. Thus, by applying a bias-field, the S-mode relaxation frequency and dielectric strength are observed near the SmC*–SmA phase transition region in the SmC* phase. The dependences of the relaxation frequency (v) and the inverse of dielectric strength ($\Delta\varepsilon^{-1}$) on temperature for a fixed bias-field strength of 15 V are shown in figure 7. It can be seen that a ferroelectric second-order [13, 35] SmA–SmC* phase transition occurs at $T_C \sim 132.9°C$, at which the V-shaped plots of v and $\Delta\varepsilon^{-1}$ versus temperature are minimized. These results can be explained on the basis of the standard molecular-field approximation [11, 36]

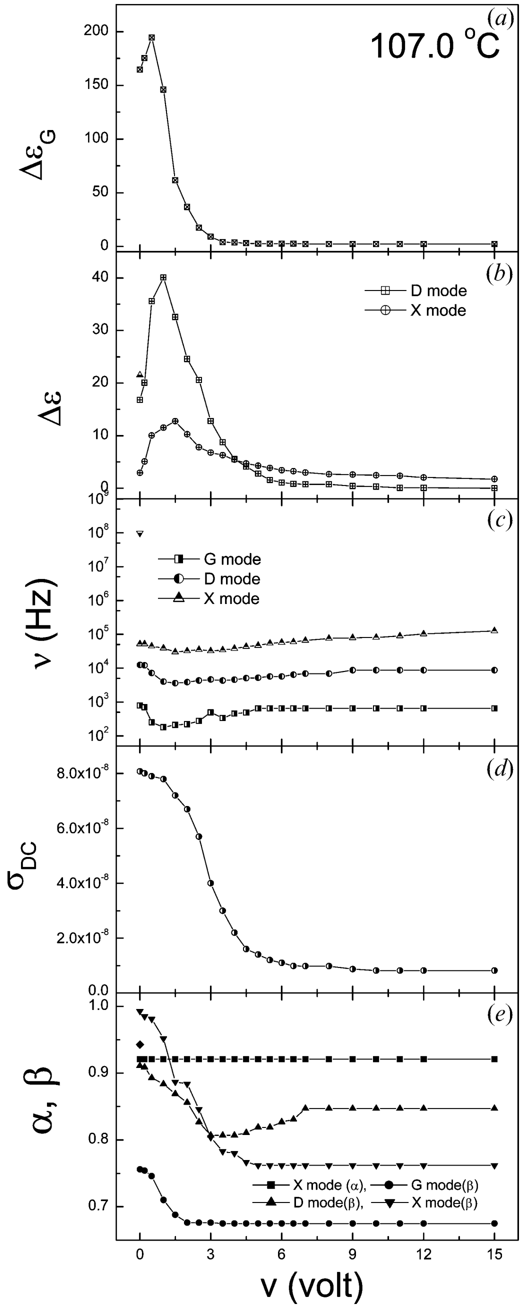

Figure 6. Variations of (a, b) dielectric strength ($\Delta\varepsilon$) for different relaxation modes, (c) relaxation frequency (ν) of different relaxation modes, (d) dc conductivity (σ_{dc}) and (e) symmetric (β) and asymmetric (α) parameters for different relaxation modes with bias-field at fixed temperature of 107°C in the SmC* phase.

for the SmA–SmC* phase transition, which predicts the following behaviour of the S-mode for the SmA phase:

$$\upsilon_{SA} \approx A(T - T_C) + Bq_0^2, \tag{3a}$$

$$\varepsilon_0 \Delta\varepsilon_{SA} \approx \frac{1}{A(T - T_C) + Bq_0^2}, \tag{3b}$$

where A and B are constants of the model and q_0 is the wavevector of the pitch at T_C. In the SmC* phase, the S-mode parameters are given by equations (3a) and (3b), replacing $A(T-T_C)$ by $2A(T-T_C)$.

According to this approximation, the critical frequency and the dielectric strength of the S-mode should follow equation (3) and their slope ratio is predicted to be 2. The ratio of the slopes of the fitted straight lines in figure 7a is about 2.15 for the relaxation frequency, roughly 7.8% higher than the corresponding theoretical value. The slope ratio for the inverse of the dielectric strength (figure 7b), is 2.01, about 0.3% lower than the corresponding theoretical value. Hence, the frequency and the inverse of the dielectric strength of the S-mode extrapolated to the transition temperature at zero momentum transfer (q=0) have a finite value and this supports the theory [37].

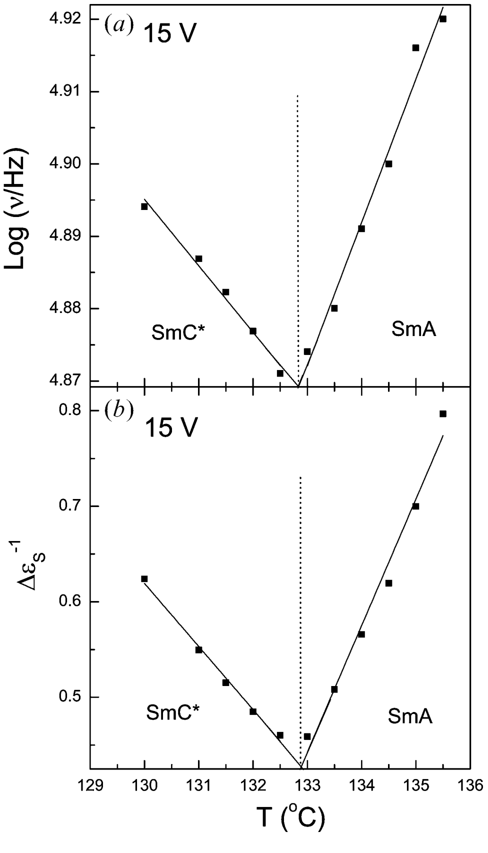

Figure 7. Temperature dependences of S-mode relaxation frequency (a) and inverse of dielectric strength (b) in vicinity of the SmA–SmC* transition in SmA and SmC* phases for bias-field of 15 V.

4. Conclusions

The temperature- and frequency-dependent dielectric constants of the FLC system clearly showed successive phase transitions from crystalline to isotropic phases. These phase transitions were observed very clearly from the study of the temperature dependence of the symmetric and asymmetric parameters and also from the conductivity contribution calculated from equation (1). We have reported the variation of the symmetric and asymmetric parameters and also the conductivity contribution from temperature and bias-field. Comparing the experimental data with theoretical calculations, we have analysed the complex dielectric behaviour in the SmX–SmC* and SmC*–SmA transition regions. In the SmX and SmC* phases, we have observed two symmetric modes (G-mode and D-mode) and in the SmC*, SmA and isotropic phases, we have observed only the X-mode (asymmetric). In the ferroelectric SmC* phase, a very large contribution of the electric permittivity is observed, which is assigned the G-mode. It is noticed that the G-mode is strongly bias-field dependent and it practically disappears by applying higher fields. By applying a bias-field, the G-mode character decreases and the D-mode is now visible. The effects of the bias-voltage on the S-mode dielectric relaxation process have been examined.

Acknowledgements

This work was supported by the Japan Society for the promotion of Science (JSPS), Japan (No. 17-05061).

References

[1] S.T. Lagerwall, B. Otterholm, K. Sharp. *Mol. Cryst. liq. Cryst.*, **152**, 503 (1987).
[2] L.A. Beresnev, L.A. Blinov, M.A. Osipov, S.A. Pikin. *Mol. Cryst. liq. Cryst.*, **158**, 1 (1988).
[3] R. Blinc, C. Filipic, A. Levstik, B. Zeks. *Mol. Cryst. liq. Cryst.*, **151**, 1 (1987).
[4] N.A. Clark, S.T. Lagerwall. *Appl. Phys. Lett.*, **36**, 879 (1980).
[5] M. Marzec, M. Godlewska, W. Haase, S. Hiller, S. Wrobel. *Mol. Mater.*, **6**, 261 (1996).
[6] S.V. Yablonskii, T. Weyrauch, W. Haase, S. Ponti, A. Strigazzi, C.A. Veracini, C. Gandolfo. *Ferroelectrics*, **188**, 175 (1996).
[7] B. Palacios, M.R. de la Fuente, M.A.P. Jubindo, M.B. Ros. *Liq. Cryst.*, **23**, 349 (1997).
[8] A. Levstik, T. Carlsson, C. Filipic, I. Levstik, B. Zeks. *Phys. Rev. A*, **35**, 3527 (1987).
[9] L.A. Beresnev, M. Pfeiffer, S.A. Pikin, W. Haase, L.A. Blinov. *Ferroelectrics*, **132**, 99 (1992).
[10] S. Hiller, L.A. Beresnev, S.A. Pikin, W. Haase. *Ferroelectrics*, **180**, 727 (1996).
[11] T. Carlsson, B. Zeks, C. Filipic, A. Levstik. *Phys. Rev. A*, **42**, 877 (1990).
[12] S.K. Kundu, K. Suzuki, B.K. Chaudhuri. *J. appl. Phys.*, **94**, 2271 (2003).
[13] S.K. Kundu, B.K. Chaudhuri, L. Catala, S. Mery. *Liq. Cryst.*, **29**, 837 (2002).
[14] S. Merino, F. de Daran, M.R. de la Fuente, M.A.P. Jubindo, T. Sierra. *Liq. Cryst.*, **23**, 275 (1997).
[15] L. Benguigui. *J. Phys., Paris*, **43**, 915 (1982).
[16] S. Merino, M.R. de la Fuente, Y. González, M.A.P. Jubindo, B. Ros, J.A. Puertolas. *Phys. Rev. E*, **54**, 5169 (1996).
[17] Y. González, B. Palacios, M.A.P. Jubindo, M.R. de la Fuente, J.L. Serrano. *Phys. Rev. E*, **52**, R5764 (1995).
[18] W.L. Tsai, F.M. Hsu, J.N. Chen. *Liq. Cryst.*, **31**, 299 (2004).
[19] J. Mieczkowski, E. Gorecka, D. Pociecha, M. Glogarova. *Ferroelectrics*, **212**, 357 (1998).
[20] E. Gorecka, J. Mieczkowski, L. Chen. *Liq. Cryst.*, **23**, 185 (1997).
[21] L.A. Blinov, T.A. Lobko, B.I. Ostrovskii, S.N. Sulianov, F.G. Toumilhac. *J. Phys., Paris II*, **3**, 1211 (1993).
[22] V. Novotna, M. Kaspar, V. Hamplova, M. Glogarova, I. Rychetsky, D. Pociecha. *Liq. Cryst.*, **31**, 1131 (2004).
[23] K. Ema, H. Yao, Y. Takanishi, H. Takezoe, T. Kusumoto, T. Hiyama, A. Yoshizawa. *Liq. Cryst.*, **29**, 221 (2002).
[24] S.S. Seomun, T. Gouda, Y. Takanishi, K. Ishikawa, H. Takezoe, A. Fukuda. *Liq. Cryst.*, **26**, 151 (1999).
[25] S.-L. Wu, C.-Y. Lin. *Liq. Cryst.*, **32**, 663 (2005).
[26] S. Wrobel, A. Fafara, W. Haase, D. Kilian, H.T. Nguyen, K. Saxena. *Proc. SPIE*, **3318**, 128 (1998).
[27] N. Shiratori, I. Nishiyama, A. Yashizawa, T. Hirai. *Jap. J. appl. Phys.*, **29**, L2086 (1990).
[28] S. Havriliak, S. Negami. *J. Polym. Sci.*, **14**, 99 (1966).
[29] S.A. Rozanski, R. Stannarius, F. Kremer, S. Diele. *Liq. Cryst.*, **28**, 1071 (2001).
[30] R.J. Cava, J.S. Patel, K.R. Collen, J.W. Goodby, E.A. Rietman. *Phys. Rev. A*, **35**, 4378 (1987).
[31] S. Mashimo, R. Nozaki, S. Yagihara, S. Takeishi. *J. chem. Phys.*, **77**, 6259 (1982).
[32] S. Sudo, S. Tsubotani, M. Shimomura, N. Shinyashiki, S. Yagihara. *J. chem. Phys.*, **121**, 7332 (2004).
[33] S.K. Kundu, K. Suzuki, B.K. Chaudhuri. *Ferroelectrics*, **287**, 47 (2003).
[34] A. Kocot, R. Wrzalik, J.K. Vij, M. Brehmer, R. Zentel. *Phys. Rev. B*, **50**, 16346 (1994).
[35] H. Xu, J.K. Vij, A. Rappaport, N.A. Clark. *Phys. Rev. Lett.*, **79**, 249 (1997).
[36] T. Carlsson, B. Zeks, A. Levstik, C. Filipic, I. Levstik, R. Blinc. *Phys. Rev. A*, **36**, 1484 (1987).
[37] R. Blinc, B. Zeks. *Phys. Rev. A*, **18**, 740 (1978).